PHOTOSYNTHETICA
International Journal for Photosynthesis Research

DOI 10.32615/ps.2023.016 PHOTOSYNTHETICA 61 (3): 275-284, 2023

Changes of dorsoventral asymmetry and anoxygenic photosynthesis in response of *Chelidonium majus* leaves to the SiO_2 nanoparticle treatment

V. LYSENKO[*,+], Y. GUO[**], V.D. RAJPUT[*], E. CHALENKO[*], O. YADRONOVA[*], T. ZARUBA[*], T. VARDUNY[*], and E. KIRICHENKO[*]

Academy of Biology and Biotechnology, Southern Federal University, Rostov-on-Don, Russia[*]
Key Laboratory of Advanced Process Control for Light Industry, Jiangnan University, Wuxi, China[**]

Abstract

Natural SiO_2 nanoparticles (SiO_2-NPs) are widely distributed in the environment, and at the same time, synthetic SiO_2-NP may be applied in agriculture. Evaluations of physiological responses to SiO_2-NPs treatment of plants are controversial. They are often performed at adaxial leaf sides whereas NPs permeate leaf tissues through stomata located at the abaxial leaf side in the majority of bifacial plants. We measured coefficients of the functional dorsoventral asymmetry of NPs-stressed *Chelidonium majus* leaves, S, by values of the CO_2 assimilation rate (SP_N), dark respiration (SR), maximal and operating quantum yields of photosystem II (SF_v/F_m, SF_v'/F_m'; using PAM-fluorometry), and oxygen coefficients of photosynthesis ($S\Psi_{O2}$; using photoacoustics). The results indicated that SP_N and $S\Psi_{O2}$ were significantly influenced by SiO_2-NPs treatment, since P_N and Ψ_{O2} were declining more markedly when the light was directed to the abaxial side of leaves compared to the adaxial side. Overall, SiO_2-NPs-induced stress increased 'anoxygenity' of photosynthesis.

Keywords: CO_2 assimilation kinetics; cyclic electron transport around PSII; energy storage; photobaric signal; photothermal signal; transpiration kinetics.

Introduction

Natural and engineered silicon dioxide nanoparticles (SiO_2-NPs) are widely distributed in the environment (Janković and Plata 2019). Soil and foliar application of SiO_2-NPs in a wide range of concentrations (0.1–10 mg kg^{-1} of soil and 10–2,000 mg L^{-1} of foliar spray) and sizes (10–1,000 nm) are useful in agriculture for improving photosynthetic performance and yield of plants (Rastogi *et al*. 2019, Rajput *et al*. 2021). Tian *et al*. (2020) reported that foliar application of SiO_2-NPs at a concentration of 100 mg L^{-1} did not influence the photosynthesis of pakchoi plants or their biomass. However, SiO_2-NPs may have a toxic effect in conditions of soil application on *Arabidopsis*

Highlights

- SiO_2 nanoparticles (SiO_2-NPs) increased functional dorsoventral asymmetry of leaves
- A novel method of Fourier photoacoustics was applied to evaluate plant stress
- SiO_2-NPs influence 'anoxygenity' and oxygen coefficients of photosynthesis

Received 18 December 2022
Accepted 6 April 2023
Published online 12 May 2023

[+]Corresponding author
e-mail: vs958@yandex.ru

Abbreviations: CET-PSI and CET-PSII – cyclic electron transport around PSI and II, respectively; F_v/F_m – maximal quantum yield of PSII for the dark-adapted states; F_v'/F_m' – operating quantum yield of PSII for the light-adapted states; LED – light-emitting diode; PA – photoacoustic; PA_{ac280} – actual photoacoustic signal at 280 Hz detected under measuring and actinic light 2 s before the saturating flash; PA_{sat280} – photoacoustic signal at 280 Hz detected under measuring light and saturating flash; P_N – CO_2 assimilation rate; R – dark respiration rate; SiO_2-NPs – silicon dioxide nanoparticles; SP – coefficient of dorsoventral asymmetry calculated based on CO_2 assimilation rates; $S\Psi_{O2}$ – coefficient of dorsoventral asymmetry calculated based on oxygen coefficients of photosynthesis; Ψ_{O2} – oxygen coefficient of photosynthesis.

Acknowledgments: The project was supported by the Russian Science Foundation under Grant No. 22-14-00338, https://rscf.ru/project/22-14-00338/, and performed at Southern Federal University (Rostov-on-Don, Russian Federation).
Conflict of interest: The authors declare that they have no conflict of interest.

thaliana at concentrations of 250 and 1,000 mg L^{-1} (Slomberg and Schoenfisch 2012) and on cotton plants at concentrations in the range of 10–2,000 mg L^{-1} (Le *et al.* 2014). The toxicity of SiO_2-NPs has been also revealed in several studies on algae growth and photosynthesis (Wei *et al.* 2010, Manzo *et al.* 2015, Liu *et al.* 2018, Shariati and Shirazi 2019).

SiO_2-NPs, as well as other NPs, influence light (primary) reactions of photosynthesis (Tian *et al.* 2020, Zahedi *et al.* 2020, Li *et al.* 2021) which involves thylakoidal electron transport (ET) chain represented by PSI and PSII functioning (Stirbet *et al.* 2020).

The maximal quantum yield of PSII for the dark-adapted states (F_v/F_m) or(and) operating quantum yield of PSII for the light-adapted states (F_v'/F_m') (Schreiber 2004) are often used as the main parameters characterizing the photosynthetic performance of plants. Both these parameters are studied during physiological and toxicological experiments, including studies on the effects caused by SiO_2-NPs (Hassan *et al.* 2021, Li *et al.* 2021, Alam *et al.* 2022). Values of F_v/F_m, F_v'/F_m', and other related photosynthetic parameters of vascular plants are measured by default from the adaxial leaf side, if not specified otherwise. At the same time, in none of the carried-out studies, these photosynthetic parameters were measured from the abaxial side of the SiO_2-NPs treated leaves. However, it is evident and well-known (El-Shetehy *et al.* 2021) that NPs (if sprayed) penetrate mesophyll tissues mainly through the stomata which are located on the abaxial leaf side in most plants. Penetration of hydrophilic NPs into leaves from the adaxial side may be hindered by the presence of a wax cuticular layer (Barkataki and Singh 2019). The tissue on the abaxial side comprises the spongy mesophyll having large intercellular spaces. When moving across spongy mesophyll, NPs have a high probability of interacting with spongy mesophyll cells that prevent their interaction with the upper cells of the palisade mesophyll (Gordiichuk *et al.* 2021, Ballikaya *et al.* 2023). Therefore, it cannot be excluded that the NPs-induced stress may, at least in some cases, affect mainly the spongy mesophyll, while photosynthetic parameters are usually measured from the palisade mesophyll.

Even when ignoring the spatial direction (from the adaxial or abaxial side) of stressor action, differential evaluation of the stress-induced dysfunction of the palisade and spongy mesophyll is important because of the differences in their anatomy (Oguchi *et al.* 2018). Thus, the anatomical characteristics mentioned above evidently suggest better CO_2 access to the cells of the spongy mesophyll compared to the palisade mesophyll. The paradox here is that the palisade mesophyll adsorbs a significantly higher proportion of incident light than the spongy mesophyll by a factor of 5–20 (Hagemeier and Leuschner 2019).

In this regard, it is of interest that there was no difference in CO_2 assimilation rates between the adaxial and abaxial sides of *Paspalum dilatatum* leaves when a low PPFD [50–400 μmol m^{-2} s^{-1}] was applied (Soares *et al.* 2008). Under high, photoinhibition levels of PPFD [800–1,400 μmol m^{-2} s^{-1}], CO_2 assimilation was higher when the light was directed to the abaxial side. It suggests that spongy mesophyll, in contrast to palisade mesophyll, may be better adapted to oxygenic photosynthesis, while palisade mesophyll possibly may possess an increased level of anoxygenic photosynthesis. Consequently, processes of anoxygenic photosynthesis, as well as the dorsoventral asymmetry (adaxial/abaxial side) of leaves, should be considered in the evaluation of plant stress response.

True anoxygenic photosynthesis is based on the thylakoid electron transport processes that do not lead to water photolysis and NADPH reduction (and, therefore, to carbohydrate synthesis), but maintain proton gradient and synthesize ATP molecules (phosphorylation) (Blankenship 2014). In vascular plants, this is a cyclic electron transport around PSI (CET-PSI; Munekage and Shikanai 2005) and around PSII (CET-PSII; Prasil *et al.* 1996, Johnson 2011, Lysenko and Varduny 2022). In contrast to true anoxygenic photosynthesis, quasi-anoxygenic photosynthesis comprises that part of the photosynthetic oxygen evolution that is compensated by the processes of O_2 uptake, Mehler cycle, PTOX activity, photorespiration, *etc.* (Lysenko and Varduny 2022). Unfortunately, quantification of anoxygenic photosynthesis (especially of CET-PSII) is a difficult task, because PAM-fluorometers cannot distinguish between the noncyclic and cyclic modes of the PSII activity (Lysenko *et al.* 2017). In addition, it is difficult to measure the 'pure' photosynthetic oxygen evolution, without the contribution of O_2-uptake processes. However, quantification of anoxygenic photosynthesis may be achieved using photoacoustic methods by detecting the pulse oxygen evolution (photobaric signal) excited by a pulse measuring light at low frequencies (20–40 Hz) as far as the O_2-uptake processes are continuous (non-pulsing) at these frequencies being inertial due to the buffer capacity of the molecular pools involved in them (Malkin 1996, 1998). At high frequencies (200–400 Hz), a photoacoustic spectrometer detects a photothermal signal and may measure the value of photochemically stored energy (or called simply energy storage, ES) reflecting the portion of the absorbed light energy that is utilized in the photochemical processes (Malkin 1996, 1998; Buschmann 1999). A novel method of Fourier-photoacoustics allows measuring photobaric and photothermal signals simultaneously in one sample and calculating oxygen coefficients of photosynthesis (Ψ_{O2}) (Lysenko and Varduny 2022). The value of Ψ_{O2} is proportional to the ratio between the O_2 evolution rate and ES, thus evaluating the degree of 'anoxygenity' of photosynthesis.

Until now, NPs-induced plant stress response was not studied using a complex of parameters allowing distinguishing between oxygenic and anoxygenic photosynthesis and between adaxial and abaxial application of light (regarding functions of palisade and spongy mesophyll).

In the present work, we measured coefficients of the functional dorsoventral asymmetry, S, of the normal and

NPs-stressed *C. majus* leaves based on the values of the CO_2 assimilation rate (P_N), dark respiration (R), F_v/F_m, F_v'/F_m', and Ψ_{O2}. Values of S (SP_N, SR, SF_v/F_m, SF_v'/F_m', and $S\Psi_{O2}$, respectively) were calculated as a ratio of the studied parameters measured using the adaxial light application to that of the abaxial light application.

We showed that NPs treatment significantly decreased CO_2 assimilation, P_N, and oxygen coefficients of photosynthesis, Ψ_{O2}, which were both decreased more strongly if the light was applied from the abaxial side. Thus, NPs treatment increased the functional dorsoventral asymmetry of leaves evaluated by these parameters (SP_N and $S\Psi_{O2}$). However, NPs treatment did not significantly affect the quantum yield of PSII, leaving F_v/F_m, F_v'/F_m', SF_v/F_m, and SF_v'/F_m' to be weakly changed. It may suggest that, under SiO_2-NPs treatment, some part of oxygenic photosynthesis based on thylakoid noncyclic electron transport in the *C. majus* leaves was substituted by the anoxygenic photosynthesis based on the cyclic electron transport around PSII (CET-PSII). Therefore, the photosynthetic response of plants to stress (at least in the given case) should be evaluated considering 'anoxygenity' of photosynthesis and considering the functions of palisade and spongy mesophyll.

Materials and methods

Plant material: Experiments were conducted in May on *Chelidonium majus* plants grown in the Botanical Garden of the Southern Federal University (Rostov-on-Don) in the shadow of trees. Throughout the entire period of the experiment (9 sunny days), all of the leaves at the time of cutting (from 10:00 to 22:00 h) received PPFD of approximately 70–120 µmol m^{-2} s^{-1}. Ambient daytime temperatures were about 18–21°C. All of the studied plants grew in the same soil, relief, and water conditions, *i.e.*, grey forest soil (flat area), with relative soil humidity of 45–60%. Fully developed leaves (Fig. 1) were collected from plants reaching 50–60 cm in height and were used in the experiment not later than 10 min after detaching.

C. majus is known as a shade-tolerant plant having bifacial leaves with stomata confined to the abaxial side (Zare *et al*. 2021).

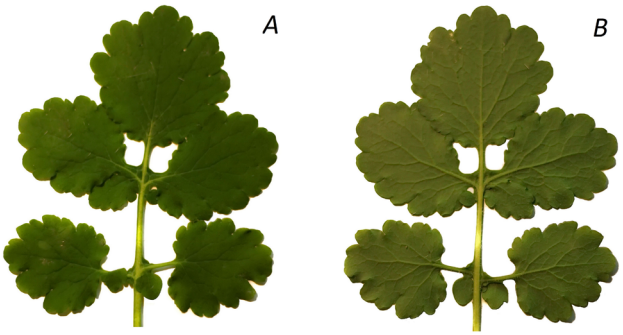

Fig. 1. A *Chelidonium majus* leaf. (*A*) adaxial side; (*B*) abaxial side.

Treatment by SiO_2 nanoparticles: Commercial grade silicon dioxide (SiO_2) NPs powder (*Sigma-Aldrich*, particle size of 10–20 nm) was suspended in distilled water to a concentration of 100 mg L^{-1}. The suspension was applied using a manual sprayer until full moisturizing of the accessible leaf surface was obtained or using vacuum infiltration. Vertically hinged leaves were sprayed from both sides once immediately after detaching. They stayed wet for 5 min and then we removed excess moisture with filter paper followed by drying in an air stream and reweighting to achieve an initial leaf mass. The air drying usually took 15–20 min. The leaves sprayed with distilled water and the leaves infiltrated with distilled water were studied as controls. Measurement of the photosynthetic parameters started 1 h after the treatment.

PAM-fluorometry: The maximal quantum yield of PSII for the dark-adapted states (F_v/F_m) and operating quantum yield of PSII for the light-adapted states (F_v'/F_m') (Schreiber 2004) were measured from adaxial and abaxial leaf sides of leaves using *DivingPAM* fluorometer (*Walz*, Germany). Measurements of the F_v/F_m values were performed after 30-min adaptation of plants in the dark, and measurements of the F_v'/F_m' values after 30-min adaptation under red actinic light [LED; λ_{max} = 635 nm; PPFD = 70 µmol m^{-2} s^{-1}], correspondingly to the lower limit of the growing PPFD range.

Photoacoustic studies: Photothermal and photobaric signals were monitored using a lab-made photoacoustic spectrometer following the novel method of double-wavelength Fourier photoacoustics described previously (Lysenko and Varduny 2022).

Leaf discs (10 mm in diameter) were cut from the leaves and were placed in an open photoacoustic cell (glass, 200 L) (Barja *et al*. 2001) in such a way that the adaxial leaf surface was turned inside the cell, and the abaxial surface was turned outside into the inner volume (200 ml) of the outer glass flask filled with wet air (relative humidity of 95%). The design of the cell (supplementary Fig. S1 in the work by Lysenko and Varduny 2022) allows for avoiding changes in the air composition during prolonged experiments.

Pulsed measuring lights of two frequencies – 20 and 280 Hz [red LEDs, 1 µmol(photon) m^{-2} s^{-1}], were applied simultaneously to one sample (leaf) to excite photobaric and photothermal signals, respectively. Saturating non-modulated light was emitted from a white 20 W LED to achieve a PPFD of 1,800 µmol m^{-2} s^{-1}. Actinic light [LED; λ_{max} = 635 nm; PPFD = 70 µmol m^{-2} s^{-1}] was switched together with measuring lights. The photoacoustic cell was communicated with an electret microphone. The microphone signal was passed through a low-noise operational amplifier, and the output signal was passed to a PC sound card. Real-time signal data processing was conducted to perform FFT using the *SpectraPlus* program package. Two frequency markers (20 Hz and 280 Hz) were selected, and the amplitude values measured at these frequencies were saved into a text log file every 0.7 s. Then, corresponding PA kinetic curves were plotted.

The following settings were applied: an FFT size of 131,072 samples, a sampling rate of 192,000 Hz, sampling format of 16 bits.

Saturating flashes of 10-s durations were applied 30 min after switching the actinic light on. The PA signal detected under measuring and actinic light (actual PA-signal) 2 s before the saturating flash was referred to as PA_{ac}. PA-signal measured under saturating flash was referred to as PA_{sat} (Fig. 2). The lowercase digits 20 and 280 (in PA_{ac280}, PA_{ac20}, PA_{sat280}, PA_{sat20}) mean the frequency of the measuring light applied.

Measuring main PA parameters: PA_{ac20} and PA_{ac280} are the PA signals induced by measuring light at 20 and 280 Hz in the presence of actinic light (actual PA-signal) 2 s before the saturating flash. PA_{sat20} and PA_{sat280} are the PA signals induced by measuring light at 20 and 280 Hz under saturating flash (SF).

Oxygen coefficients of photosynthesis were calculated as:

$$\Psi_{O2} = PA_{ac20} - PA_{sat20} + \frac{PA_{sat20}}{PA_{sat280}} \quad (1)$$

This equation considers a small addition of the photothermal signal to the photobaric signal (Lysenko and Varduny 2022).

Measurements of CO_2 assimilation rates and dark respiration: *C. majus* leaves were placed into 0.25-ml water-filled mini-tubes *via* their petioles, where they were encapsulated. Leaves with the mini-tubes were placed in a flat-parallel glass chamber (100 × 50 × 5 mm) fed by a pneumatic line communicating with a digital gas flowmeter, humidifier, gas flow stabilizer, and gas balloon with compressed air. The airflow was adjusted to 100 ml min^{-1}, and the relative air humidity was 60%. The input CO_2 concentration (Q_0) was 420 ppm. The output of the chamber was connected with a nondispersive infrared CO_2-sensor *IRM300* (*SemeaTech*, China) communicating with the PC *via* a USB port. The CO_2 concentrations were measured every 3 s for 40 min in response to switching red actinic light [80 µmol(photon) m^{-2} s^{-1}] at 10th min after the beginning of measurements (Fig. 3). The data were saved into a text log file, from which the corresponding kinetic curves were obtained.

Net CO_2 assimilation rate was calculated as:

$$P_N\ [\mu mol\ m^{-2}\ s^{-1}] = 7.44 \times 10^{-3} \times \Delta pCO_2\ [ppm] \times V_{air}\ [ml\ min^{-1}]/S_{leaf}\ [cm^2] \quad (2)$$

where ΔpCO_2 is the difference between output CO_2 concentrations in the dark (Q_R) and light (Q_P) (Fig. 2); V_{air} is an air volume flow rate; S_{leaf} is a leaf area, and 7.44×10^{-3} is a complex coefficient for conversion ppm to mol, min to s, and cm^2 to m^2.

The dark respiration rate was calculated as:

$$R\ [\mu mol\ m^{-2}\ s^{-1}] = 7.44 \times 10^{-3} \times \Delta rCO_2\ [ppm] \times V_{air}\ [ml\ min^{-1}]/S_{leaf}\ [cm^2] \quad (3)$$

where ΔrCO_2 is the difference between input (Q_0) and output (Q_R) CO_2 concentrations in the dark (*see* Fig. 2).

S_{leaf} was measured using a PC scanner and *ImageJ* software.

Calculating coefficients of functional dorsoventral asymmetry of leaves: Coefficients of the dorsoventral asymmetry (S) were proposed and calculated on the basis of CO_2 assimilation rates and on oxygen coefficients of photosynthesis (obtaining SP_N and $S\Psi_{O2}$, respectively) as a ratio of the studied parameter (P_N or Ψ_{O2}) measured using the adaxial light application to that parameter measured using the abaxial light application.

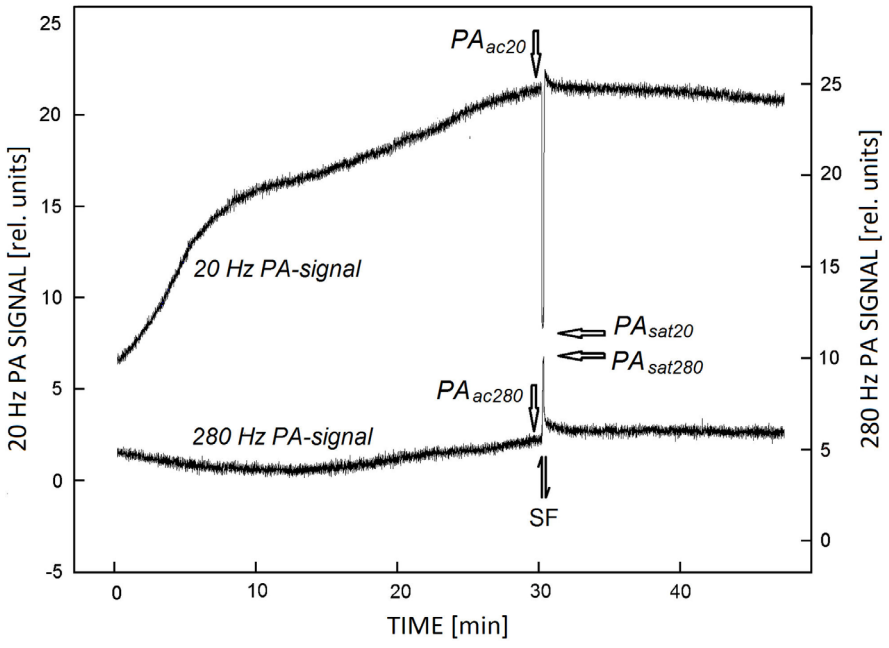

Fig. 2. Typical photoacoustic (PA) signals induced in *Chelidonium majus* leaves. Measuring main PA-parameters. PA_{ac20} and PA_{ac280} are the PA signals induced by measuring light at 20 and 280 Hz in the presence of actinic light (actual PA-signal) 2 s before the saturating flash. PA_{sat20} and PA_{sat280} are the PA signals induced by measuring light at 20 and 280 Hz under saturating flash (SF).

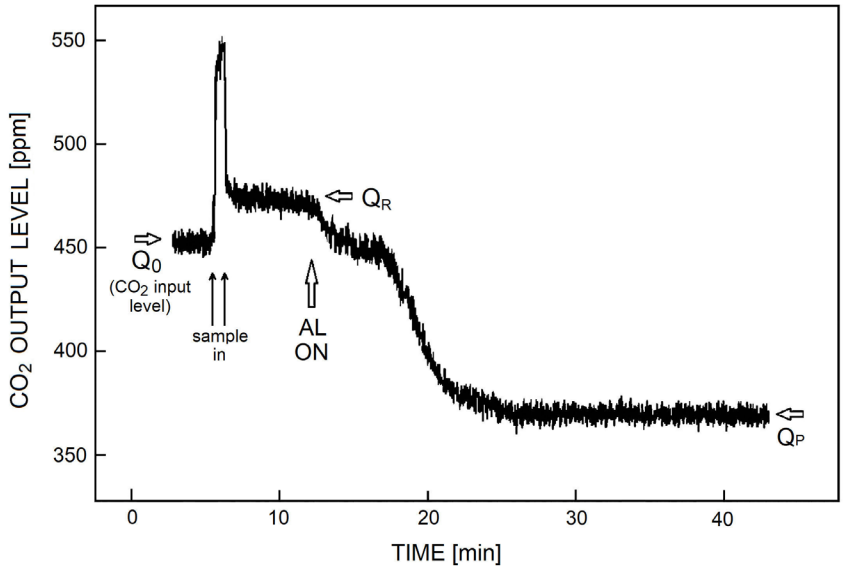

Fig. 3. Typical CO_2-assimilation kinetics measured in *Chelidonium majus* leaves in response to switching actinic light on (AL ON). Measurements of CO_2 concentrations were performed at the output of the flow cell. Q_0 – CO_2 concentration measured with empty cell equal to the input level; Q_R – CO_2 concentration measured in dark (respiration); Q_P – CO_2 concentration measured under actinic light (photosynthesis). When the samples were placed into the cell (↑↑ sample in), CO_2 concentration sharply increased due to the ambient air entering the chamber.

Adjusting photon fluxes: Levels of photosynthetic photon flux density (PPFD) were measured and adjusted using a PPFD sensor of the *DivingPAM* fluorometer (*Waltz*, Germany).

Monitoring of transpiration: The transpiration kinetics was determined using a PC-gravimetric method. *C. majus* leaves were placed into 5-ml water-filled minitubes *via* their petioles, and the open water surface was covered by silicone oil. The mounted leaf samples were continuously weighed using *AdventurerPro* analytical balances communicating with a PC. The data were saved into a text log file every 3 s. The transpiration kinetics was studied in response to switching the red actinic light [70 μmol(photon) m^{-2} s^{-1}] on and off.

Statistical analysis: Testing of statistically significant differences between the oxygen coefficients of photosynthesis Ψ_{O2}, CO_2 assimilation rates P_N, coefficients of dorsoventral asymmetry $S\Psi_{O2}$, SP_N (done by *ANOVA* test), and evaluating of mean ± SD for other parameters were performed using *Microsoft Excel 2010* software.

Results

Our data showed that there were no significant differences between whether the studied gas exchange (P_N, R), fluorescence kinetic (F_v/F_m, F_v'/F_m'), and photoacoustic (Ψ_{O2}) parameters were measured in the leaves sprayed with distilled water and in the leaves infiltrated with distilled water (Table 1). If the leaves were sprayed with SiO_2-NPs suspension, the values of quantum yield of PSII, F_v/F_m, and F_v'/F_m' remained insignificantly changed independently of which side of the leaf they were measured from. At the same time, CO_2 assimilation (P_N) and oxygen coefficients of photosynthesis (Ψ_{O2}) remained unchanged (compared with untreated control) when leaves were sprayed with SiO_2-NPs only if both these values were measured under actinic light applied from the adaxial side. However, P_N and Ψ_{O2} were found to be decreased (from 1.61 to 1.41 and from 4.5 to 4.0, respectively, with significant differences for p=0.05) by spraying leaves with SiO_2-NPs if they were measured in condition of the abaxial application of actinic light.

Infiltration with SiO_2-NPs caused a more pronounced effect on P_N and Ψ_{O2}. The P_N value significantly and strongly decreased (compared with infiltration by distilled water) independently of from which side of the leaf the actinic light was applied (adaxial: from 1.63 to 1.23; abaxial: from 1.61 to 0.69). The Ψ_{O2} values insignificantly decreased from 4.6 to 4.4 if they were measured under the adaxially directed actinic light and significantly strongly decreased from 4.0 to 2.5 when it was directed abaxially (Table 1).

If compared with infiltration with distilled water, infiltration with SiO_2-NPs did not lead to any significant decrease in the F_v/F_m and F_v'/F_m' values, both in the cases when the actinic light was directed to the adaxial and abaxial side.

The values of dark respiration (0.30) in the leaves infiltrated with SiO_2-NPs significantly decreased compared to that of the untreated leaves (0.40), the leaves infiltrated with distilled water (0.38), and leaves sprayed with SiO_2-NPs (0.37) (Table 1).

There were no significant differences in the coefficients of dorsoventral asymmetry (S) calculated based on all the studied parameters (SP_N, SR, SF_v/F_m, SF_v'/F_m', and $S\Psi_{O2}$) between whether they were measured in the untreated leaves or the leaves infiltrated with distilled water (Fig. 4). However, spraying of SiO_2-NPs suspension caused a small but statistically significant decrease in the SP_N and $S\Psi_{O2}$ values that was much more pronounced if SiO_2-NPs were applied using the infiltration. At that time, SF_v/F_m and SF_v'/F_m' were weakly influenced even in the SiO_2-NPs infiltrated leaves (Fig. 4).

Table 1. Responses of photosynthetic parameters measured from adaxial and abaxial sides of *Chelidonium majus* leaves to SiO_2-NPs treatment. SiO_2-NPs were applied at a concentration of 100 mg L^{-1} using spraying or vacuum infiltration. P_N, F_v'/F_m', and Ψ_{O2} values were measured after 30-min adaptation under red actinic light [LED; λ_{max} = 635 nm; PPFD = 70 µmol m^{-2} s^{-1}] which was turned on after 1 h of NP-treatment. *Different letters* indicate that values were significantly different at p<0.05.

Direction of actinic light	Net CO_2 assimilation, P_N [µmol(CO_2) m^{-2} s^{-1}]	Dark respiration, R [µmol(CO_2) m^{-2} s^{-1}]	Maximal quantum yield of PSII, F_v/F_m	Operating quantum yield of PSII, F_v'/F_m'	Oxygen coefficients of photosynthesis, Ψ_{O2}
Spraying with distilled water					
adaxial	1.66 ± 0.14[a]	0.40 ± 0.02[a]	0.82 ± 0.06[a]	0.30 ± 0.02[a]	4.8 ± 0.5[a]
abaxial	1.62 ± 0.13[a]		0.81 ± 0.06[a]	0.28 ± 0.02[a]	4.6 ± 0.4[a]
Vacuum infiltration with distilled water					
adaxial	1.63 ± 0.10[a]	0.38 ± 0.03[a]	0.80 ± 0.08[a]	0.29 ± 0.03[a]	4.6 ± 0.4[a]
abaxial	1.61 ± 0.09[a]		0.77 ± 0.07[a]	0.27 ± 0.03[a]	4.5 ± 0.4[a]
Spraying with SiO_2-NPs					
adaxial	1.62 ± 0.14[a]	0.37 ± 0.02[a]	0.81 ± 0.08[a]	0.29 ± 0.02[a]	4.7 ± 0.5[a]
abaxial	1.41 ± 0.13[b]		0.80 ± 0.08[a]	0.26 ± 0.02[a]	4.0 ± 0.4[a]
Vacuum infiltration with SiO_2-NPs					
adaxial	1.23 ± 0.10[c]	0.30 ± 0.04[b]	0.80 ± 0.08[a]	0.29 ± 0.03[a]	4.4 ± 0.4[a]
abaxial	0.69 ± 0.11[d]		0.77 ± 0.08[a]	0.24 ± 0.03[b]	2.5 ± 0.5[b]

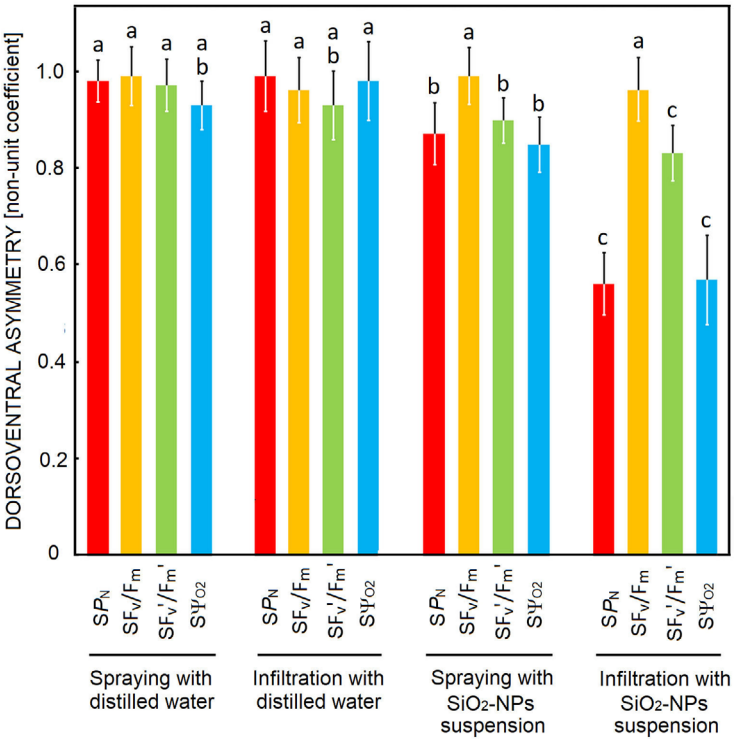

Fig. 4. Effects of SiO_2-NPs treatment on the functional dorsoventral asymmetry (S) of net CO_2 assimilation (SP_N), the maximal quantum yield of PSII (SF_v/F_m), operating quantum yield of PSII (SF_v'/F_m'), and oxygen coefficients of photosynthesis (Ψ_{O2}), calculated as a ratio between their values measured from adaxial and abaxial sides of *Chelidonium majus* leaves. Error bars are given as X ± SD for p=0.05. *Different letters* indicate that values were significantly different at p<0.05.

Studies on responses of the transpiration kinetics to switching actinic light on and off showed that the transpiration rates of the leaves infiltrated with SiO_2-NPs measured after 70 min of the experiment (the endpoint of curve 1; Fig. 5) were significantly different from that of measured for leaves sprayed with distilled water, leaves sprayed with SiO_2-NPs, and leaves infiltrated with distilled water (Fig. 5).

Discussion

The results obtained in the present work showed that SiO_2-NPs treatment may affect photosynthetic CO_2 assimilation in the short time-scale (about 1 h) experiments when applied using spraying and vacuum infiltration with SiO_2-NP suspension in the concentration of 100 mg L^{-1}. The infiltrated SiO_2-NPs caused a greater effect than

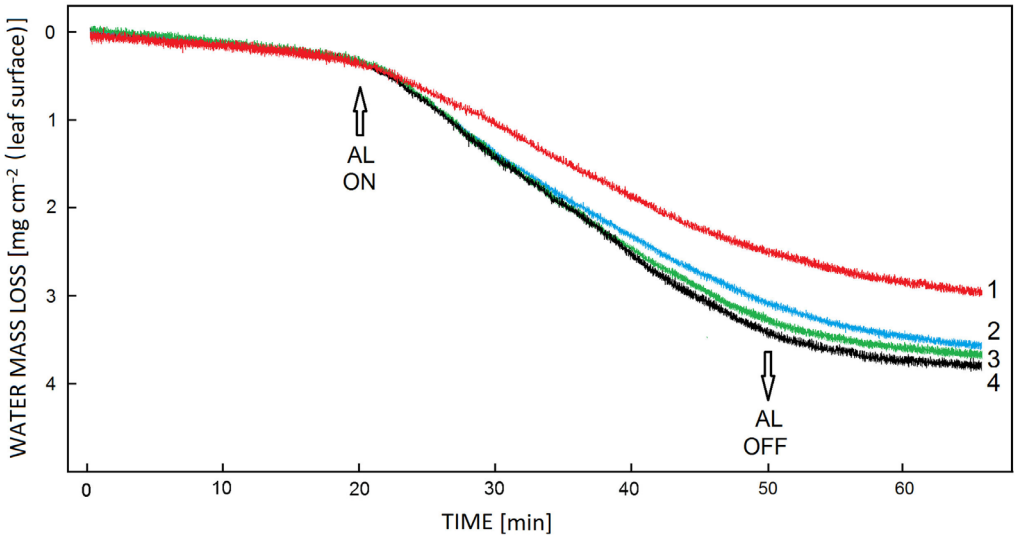

Fig. 5. Responses of transpiration kinetics of *Chelidonium majus* leaves treated with SiO_2-NPs to switching the actinic light on and off. 1 – leaves infiltrated with SiO_2-NPs suspension; 2 – leaves infiltrated with distilled water (control); 3 – leaves sprayed with SiO_2-NPs suspension; 4 – untreated leaves (control); AL ON and AL OFF – switching actinic light [red LED, 70 µmol(photon) m^{-2} s^{-1}], applied from the adaxial side) on and off. Standard deviations in the endpoints of curves (mean ± SD) are: for curve 1: 2.9 ± 0.1; for curve 2: 3.5 ± 0.1; for curve 3: 3.6 ± 0.1; for curve 4: 3.8 ± 0.2. Differences in mean values between the leaves infiltrated with SiO_2-NPs suspension (curve 1) and three other variants (curves 2–4) are statistically significant (p<0.01).

the sprayed SiO_2-NPs which was quite expected if assuming easy and increased stomata permeation of the NPs into the leaf tissues under pressure.

The negative effects of SiO_2-NPs on plants revealed in this work are consistent with the data showing that SiO_2-NPs have toxic effects on plants estimated by a decrease in their biomass, plant height, and other vegetation parameters (Le *et al*. 2014).

Nevertheless, we found that maximal and operating quantum yields of PSII (F_v/F_m, F_v'/F_m') were not significantly affected along with the decrease in the CO_2 assimilation rates. It is also consistent with the data demonstrating the absence of adverse effects of the foliar spraying of SiO_2-NPs on F_v/F_m and F_v'/F_m' (Tian *et al*. 2020). The discrepancy between the high quantum yield of PSII and low CO_2 assimilation can be explained in two ways: (*1*) an increase in the CO_2 concentrations due to the increase in CO_2-emitting processes (respiration or photorespiration), not to the decrease in photosynthesis; (*2*) functioning of some part of PSII was not accompanied with photosynthetic CO_2 assimilation that may be a result of the true anoxygenic photosynthesis (cyclic electron transport, CET-PSII) or quasi-anoxygenic photosynthesis (PTOX activity, Mehler cycle; *see* 'Introduction'). To distinguish between these two cases (1 and 2), we applied a dual wave Fourier photoacoustics, calculating oxygen coefficients of photosynthesis, Ψ_{O2}, which are based on the measurement of the parameter of a 'pure' photolytic oxygen evolution and are not influenced by respiration, photorespiration, and quasi-anoxygenic photosynthesis. We showed that under SiO_2-NP treatment, CO_2 assimilation rates in leaves decreased as well as the rates of 'pure' O_2 evolution estimated per energy utilized in the photosynthesis (Ψ_{O2}). It means (considering high F_v/F_m and F_v'/F_m') that the observed SiO_2-NP-induced decrease in CO_2 assimilation occurred in parallel to the decrease in water photolysis rates and was accompanied by high PSII activity. It may be due to only one known process – CET-PSII. All the other known processes of anoxygenic photosynthesis may only compensate for photolytic oxygen evolution but they are not related to its decline (Lysenko *et al.* 2022). Thus, the Mehler cycle (Curien *et al.* 2016), plastid terminal oxidase (PTOX) activity (Nawrocki *et al.* 2015), and rerouting of reducing power to mitochondria (Rochaix 2011) do not result in the CO_2 assimilation and O_2 evolution, but these pathways are based on the electron transport through PSII including the electron transport chain segment responsible for the water photolysis (oxygen-evolving complex, OEC). In contrast, the CET-PSII pathway bypasses OEC, although it also goes through PSII.

In any case, SiO_2-NP treatment led to the enhancement of the 'anoxygenity' of photosynthesis. It is intriguing in this connection, that CET-PSII is a relatively poorly studied process, which is possibly being underestimated at that time (Lysenko and Varduny 2022). The results obtained in this research are in agreement with the limited number of works which show the stress-response functions of CET-PSII as well as of CET-PSI. Thus, Pshibytko *et al.* (2003) measured redox potentials for plastoquinones, cytochrome *f*, and cytochrome b_{559} upon senescence, hyperthermia, and water deficit in the *Hordeum vulgare* leaves of various ages and proposed that stress activates CET-PSII.

Zhori *et al.* (2015) studied OJIP fluorescence kinetics in the fungus-infected leaves of *Euphorbia cyparissias*

calculating the photosynthetic performance index (PI), which allows for evaluating the photosynthetic electron transport beyond Q to PSI. In the infected leaves, PI strongly dropped, but F_v/F_m values were weakly affected. Therefore, the total electron transport through PSII remained relatively high, whereas electron transport through PSI was strongly decreased. It suggests an increase in the CET-PSII activity in response to infection.

Similar to CET-PSII, the CET-PSI pathway may also participate in the ATP supply in conditions of elevated ATP demand caused by temperature and water stress (Rumeau *et al.* 2007). Enhancement of both CET-PSII and CET-PSI under stress is following the common concept envisaging the elevated ATP consumption in the stressed plants which retarded their growth (Rumeau *et al.* 2007, Fraire-Velázquez *et al.* 2013, Zhang *et al.* 2020).

In addition, our results showed that CO_2 assimilation rates (P_N) and oxygen coefficients of photosynthesis (Ψ_{O2}) under SiO_2-NP treatment decreased more markedly if the actinic light was directed from the abaxial side compared to that directed from the adaxial side. We assume it might be the case if SiO_2-NPs penetrate mesophyll tissue mainly through the stomata thus firstly achieving the spongy mesophyll cells. Theoretically, in this case (if so), spongy mesophyll may be affected by SiO_2-NPs stronger than the palisade mesophyll.

From another point of view, SiO_2-NP-affected palisade mesophyll (as measured from the adaxial side) lowered values of P_N and Ψ_{O2} compared to that of spongy mesophyll along with insignificantly changed F_v/F_m and F_v'/F_m' in both kinds of mesophyll tissues. Therefore, it means that, although both palisade and spongy mesophyll possess elevated anoxygenic photosynthesis under SiO_2-NP treatment, palisade mesophyll demonstrates higher 'anoxygenity' (possibly CET-PSII) compared to the spongy mesophyll. This is in good agreement with the fact that palisade mesophyll absorbs 5–20 times more quanta of light than spongy mesophyll (Hagemeier and Leuschner 2019), being at greater risk of photoinhibition, while CET-PSII is just a mechanism for protection against photoinhibition (Allakhverdiev *et al*. 1997).

However, we understand that this interpretation of the dorsoventral asymmetry in terms of photoinhibition would appear to be simplistic. Particularly, in the natural environment (wind), plants may receive fluctuating light, some portion of which may fall directly on the abaxial leaf side even if the leaf belongs to a bifacial plant. Moreover, fluctuating light induces a rather specific photosynthetic response compared to continuous light (Lazár *et al*. 2022). It means that the problem of 'side-to-side' interactions in leaves is much more complicated than previously thought, no matter, whether it concerns normal or stressed plants.

We do not exclude that SiO_2-NP-induced mitigation of oxygenic photosynthesis found in the present study may be at least partially caused by the malfunction of the light-induced stomata opening that has been revealed from the CO_2-assimilation kinetics. Thus, it was shown using transmission electron microscopy that foliar application of SiO_2-NPs might destroy the function of stomatal cells in rice plants (Du *et al.* 2022). In addition, scanning electron microscopy showed the absorption of SiO_2-NPs by stomatal apertures in the leaves of tomato plants (Parveen and Siddiqui 2022). Hypothetically, possible consequences of this may lead to the inefficiency in stomata opening and hamper CO_2 access to mesophyll thus restricting oxygenic photosynthesis.

Conclusion: PAM-fluorometry, Fourier photoacoustic method, measurements of values of CO_2 assimilation rates (P_N), quantum yields of photosystem II (F_v/F_m and F_v'/F_m') and oxygen coefficients of photosynthesis (Ψ_{O2}) were applied to evaluate consequences of SiO_2-NP-induced stress in *C. majus* plants. The data obtained suggest the following:

(*1*) Spraying of *C. majus* leaves with SiO_2-NPs suspension has a small effect on photosynthesis whereas infiltration with SiO_2-NPs elicits a strong effect. Treatment with SiO_2-NPs causes a decrease in CO_2 assimilation and photolytic oxygen evolution. It weakly influences photosystem II activity and, therefore, increases anoxygenic photosynthesis which is most probably a consequence of the increased cyclic electron transport around PSII.

(*2*) Treatment with SiO_2-NPs causes an increase in the functional dorsoventral asymmetry of leaves estimated by the values of P_N, Ψ_{O2}, and caused enhancing the asymmetry in the activity of the anoxygenic photosynthesis.

Therefore, in studies on the SiO_2-NPs-induced plant stress, attention should be paid to the processes of anoxygenic photosynthesis, particularly to the cyclic electron transport around PSII. In addition, evaluating the consequences of NPs-induced stress on plants should be performed by measuring photosynthetic parameters from both the adaxial and abaxial sides of leaves.

References

Alam P., Arshad M., Al-Kheraif A.A. *et al.*: Silicon nanoparticle-induced regulation of carbohydrate metabolism, photosynthesis, and ROS homeostasis in *Solanum lycopersicum* subjected to salinity stress. – ACS Omega **7**: 31834-31844, 2022.

Allakhverdiev S.I., Klimov V.V., Carpentier R.: Evidence for the involvement of cyclic electron transport in the protection of photosystem II against photoinhibition: influence of a new phenolic compound. – Biochemistry **36**: 4149-4154, 1997.

Ballikaya P., Mateos J.M., Brunner I. *et al.*: Detection of silver nanoparticles inside leaf of European beech (*Fagus sylvatica* L.). – Front. Environ. Sci. **10**: 1107005, 2023.

Barja P.R., Mansanares A.M., Da Silva E.C. *et al.*: A photosynthetic induction in *Eucalyptus urograndis* seedlings and cuttings measured by an open photoacoustic cell. – Photosynthetica **39**: 489-495, 2001.

Barkataki M.P., Singh T.: Plant-nanoparticle interactions: Mechanisms, effects, and approaches. – In: Verma S.K., Das A.K. (ed.): Comprehensive Analytical Chemistry. Vol. 87. Engineered Nanomaterials and Phytonanotechnology: Challenges for Plant Sustainability. Pp. 55-83. Elsevier, Amsterdam 2019.

Blankenship R.E.: Molecular Mechanisms of Photosynthesis. 2nd Edition. Pp. 312. Wiley Blackwell, Chichester 2014.

Buschmann C.: Thermal dissipation related to chlorophyll

fluorescence and photosynthesis. – Bulg. J. Plant Physiol. **25**: 77-88, 1999.
Curien G., Flori S., Villanova V. *et al*.: The water to water cycles in microalgae. – Plant Cell Physiol. **57**: 1354-1363, 2016.
Du J., Liu B., Zhao T. *et al*.: Silica nanoparticles protect rice against biotic and abiotic stresses. – J. Nanobiotechnol. **20**: 197, 2022.
El-Shetehy M., Moradi A., Maceroni M. *et al*.: Silica nanoparticles enhance disease resistance in *Arabidopsis* plants. – Nat. Nanotechnol. **16**: 344-353, 2021.
Fraire-Velázquez S., Balderas-Hernández V.E.: Abiotic stress in plants and metabolic responses. – In: Vahdati K., Leslie C. (ed): Abiotic Stress: Plant Responses and Applications in Agriculture. Pp. 25-48. InTech Open Science, New York 2013.
Gordiichuk P., Coleman S., Zhang G. *et al*.: Augmenting the living plant mesophyll into a photonic capacitor. – Sci. Adv. **7**: eabe9733, 2021.
Hagemeier M., Leuschner C.: Leaf and crown optical properties of five early-, mid- and late-successional temperate tree species and their relation to sapling light demand. – Forests **10**: 925, 2019.
Hassan H., Alatawi A., Abdulmajeed A. *et al*.: Roles of Si and SiNPs in improving thermotolerance of wheat photosynthetic machinery via upregulation of PsbH, PsbB and PsbD genes encoding PSII core proteins. – Horticulturae **7**: 16, 2021.
Janković N.Z., Plata D.L.: Engineered nanomaterials in the context of global element cycles. – Environ. Sci.-Nano **6**: 2697-2711, 2019.
Johnson G.N.: Physiology of PSI cyclic electron transport in higher plants. – BBA-Bioenergetics **1807**: 384-389, 2011.
Lazár D., Niu Y., Nedbal L.: Insights on the regulation of photosynthesis in pea leaves exposed to oscillating light. – J. Exp. Bot. **73**: 6380-6393, 2022.
Le V.N., Rui Y., Gui X. *et al*.: Uptake, transport, distribution and Bio-effects of SiO_2 nanoparticles in Bt-transgenic cotton. – J. Nanobiotechnol. **12**: 50, 2014.
Li S., Liu J., Wang Y. *et al*.: Comparative physiological and metabolomic analyses revealed that foliar spraying with zinc oxide and silica nanoparticles modulates metabolite profiles in cucumber (*Cucumis sativus* L.). – Food Energ. Secur. **10**: e269, 2021.
Liu Y., Wang S., Wang Z. *et al*.: TiO_2, SiO_2 and ZrO_2 nanoparticles synergistically provoke cellular oxidative damage in freshwater microalgae. – Nanomaterials **8**: 95, 2018.
Lysenko V., Guo Y., Chugueva O.: Cyclic electron transport around photosystem II: mechanisms and methods of study. – Am. J. Plant Physiol. **12**: 1-9, 2017.
Lysenko V., Rajput V.D., Singh R.K. *et al*.: Chlorophyll fluorometry in evaluating photosynthetic performance: key limitations, possibilities, perspectives and alternatives. – Physiol. Mol. Biol. Pla. **28**: 2041-2056, 2022.
Lysenko V., Varduny T.: High levels of anoxygenic photosynthesis revealed by dual-frequency Fourier photoacoustics in *Ailanthus altissima* leaves. – Funct. Plant Biol. **49**: 573-586, 2022.
Malkin S.: The photoacoustic method in photosynthesis – monitoring and analysis of phenomena which lead to pressure changes following light excitation. – In: Amesz J., Hoff A.J. (ed.): Biophysical Techniques in Photosynthesis. Pp. 191-206. Springer, Dordrecht 1996.
Malkin S.: Attenuation of the photobaric-photoacoustic signal in leaves by oxygen-consuming processes. – Israel J. Chem. **38**: 261-268, 1998.
Manzo S., Buono S., Rametta G. *et al*.: The diverse toxic effect of SiO_2 and TiO_2 nanoparticles toward the marine microalgae *Dunaliella tertiolecta*. – Environ. Sci. Pollut. R. **22**: 15941-15951, 2015.
Munekage Y., Shikanai T.: Cyclic electron transport through photosystem I. – Plant Biotechnol. **22**: 361-369, 2005.
Nawrocki W.J., Tourasse N.J., Taly A. *et al*.: The plastid terminal oxidase: its elusive function points to multiple contributions to plastid physiology. – Annu. Rev. Plant Biol. **66**: 49-74, 2015.
Oguchi R., Onoda Y., Terashima I., Tholen D.: Leaf anatomy and function: including bioenergy and related processes. – In: Adams III W.W., Terashima I. (ed.): The Leaf: A Platform for Performing Photosynthesis. Pp. 97-139. Springer, Cham 2018.
Parveen A., Siddiqui Z.A.: Impact of silicon dioxide nanoparticles on growth, photosynthetic pigments, proline, activities of defense enzymes and some bacterial and fungal pathogens of tomato. – Vegetos **35**: 83-93, 2022.
Prasil O., Kolber Z., Berry J.A., Falkowski P.G.: Cyclic electron flow around photosystem II *in vivo*. – Photosynth. Res. **48**: 395-410, 1996.
Pshibytko N.L., Kalitukho L.N., Kabashnikova L.F.: Effects of high temperature and water deficit on photosystem II in *Hordeum vulgare* leaves of various ages. – Russ. J. Plant Physiol. **50**: 44-51, 2003.
Rajput V., Minkina T., Feizi M. *et al*.: Effects of silicon and silicon-based nanoparticles on rhizosphere microbiome, plant stress and growth. – Biology **10**: 791, 2021.
Rastogi A., Tripathi D.K., Yadav S. *et al*.: Application of silicon nanoparticles in agriculture. – 3 Biotech **9**: 90, 2019.
Rochaix J.-D.: Regulation of photosynthetic electron transport. – BBA-Bioenergetics **1807**: 375-383, 2011.
Rumeau D., Peltier G., Cournac L.: Chlororespiration and cyclic electron flow around PSI during photosynthesis and plant stress response. – Plant Cell Environ. **30**: 1041-1051, 2007.
Schreiber U.: Pulse-Amplitude-Modulation (PAM) fluorometry and saturation pulse method: an overview. – In: Papageorgiou G.C., Govindje G. (ed.): Chlorophyll *a* fluorescence: A Signature of Photosynthesis. Pp. 279-319. Springer, Dordrecht 2004.
Shariati F., Shirazi M.A.: Effect of SiO_2 nanoparticles on chlorophyll, carotenoid and growth of green micro-algae *Dunaliella salina*. – Nanomed. Res. J. **4**: 164-175, 2019.
Slomberg D.L., Schoenfisch M.H.: Silica nanoparticle phytotoxicity to *Arabidopsis thaliana*. – Environ. Sci. Technol. **46**: 10247-10254, 2012.
Soares A.S., Driscoll S.P., Olmos E. *et al.*: Adaxial/abaxial specification in the regulation of photosynthesis and stomatal opening with respect to light orientation and growth with CO_2 enrichment in the C_4 species *Paspalum dilatatum*. – New Phytol. **177**: 186-198, 2008.
Stirbet A., Lazár D., Guo Y., Govindjee G.: Photosynthesis: basics, history and modelling. – Ann. Bot.-London **126**: 511-537, 2020.
Tian L., Shen J., Sun G. *et al*.: Foliar application of SiO_2 nanoparticles alters soil metabolite profiles and microbial community composition in the pakchoi (*Brassica chinensis* L.) rhizosphere grown in contaminated mine soil. – Environ. Sci. Technol. **54**: 13137-13146, 2020.
Wei C., Zhang Y., Guo J. *et al*.: Effects of silica nanoparticles on growth and photosynthetic pigment contents of *Scenedesmus obliquus*. – J. Environ. Sci. **22**: 155-160, 2010.
Zahedi S.M., Moharrami F., Sarikhani S., Padervand M.: Selenium and silica nanostructure-based recovery of strawberry plants subjected to drought stress. – Sci. Rep.-UK **10**: 17672, 2020.
Zare G., Diker N.Y., Arituluk Z.C., Tatli Çankaya I.I.: *Chelidonium majus* L. (*Papaveraceae*) morphology, anatomy

and traditional medicinal uses in Turkey. – Istanbul J. Pharm. **51**: 123-132, 2021.

Zhang H., Zhao Y., Zhu J.-K.: Thriving under stress: how plants balance growth and the stress response. – Dev. Cell **55**: 529-543, 2020.

Zhori A., Meco M., Brandl H., Bachofen R.: *In situ* chlorophyll fluorescence kinetics as a tool to quantify effects on photosynthesis in *Euphorbia cyparissias* by a parasitic infection of the rust fungus *Uromyces pisi*. – BMC Res. Notes **8**: 698, 2015.